HHS Public Access

Author manuscript

Birth Defects Res C Embryo Today. Author manuscript; available in PMC 2015 June 18.

Published in final edited form as:

Birth Defects Res C Embryo Today. 2013 June ; 99(2): 106–120. doi:10.1002/bdrc.21034.

Translational Paradigms in Scientific and Clinical Imaging of Cardiac Development

Chelsea L. Gregg and **Jonathan T. Butcher**

Department of Biomedical Engineering, Cornell University, Ithaca, NY

Abstract

Congenital heart defects (CHD) are the most prevalent congenital disease with 45% of deaths resulting from a congenital defect are due to a cardiac malformation. Clinically significant CHD permit survival upon birth but may become immediately life threatening. Advances in surgical intervention have significantly reduced perinatal mortality, but the outcome for many malformations is bleak. Furthermore, patients living while tolerating a CHD often acquire additional complications due to the long-term systemic blood flow changes caused by even subtle anatomical abnormalities. Accurate diagnosis of defects during fetal development is critical for interventional planning and improving patient outcomes. Advances in quantitative, multi-dimensional imaging is necessary to uncover the basic scientific and clinically relevant morphogenetic changes and associated hemodynamic consequences influencing normal and abnormal heart development. Ultrasound is the most widely used clinical imaging technology for assessing fetal cardiac development. Ultrasound-based fetal assessment modalities include M-mode, 2D, and 3D/4D imaging. These datasets can be combined with computational fluid dynamics analysis to yield quantitative, volumetric and physiological data. Additional imaging modalities, however are available to study basic mechanisms of cardiogenesis, including optical coherence tomography, micro-computed tomography, and magnetic resonance imaging. Each imaging technology has its advantages and disadvantages regarding resolution, depth of penetration, soft tissue contrast considerations, and cost. In this review, we analyze the current clinical and scientific imaging technologies, research studies utilizing them, and appropriate animal models reflecting clinically relevant cardiogenesis and cardiac malformations. We conclude with discussing the translational impact and future opportunities for cardiovascular development imaging research.

1.0 Introduction

Congenital heart defects (CHD) are the most common congenital disease (Yang, Khoury et al. 1997) with estimated incidence rates as high as 10 in 1000 live births (Hoffman and Kaplan 2002). Furthermore, 45% of deaths resulting from a congenital defect are due to a cardiac malformation (Yang, Khoury et al. 1997). CHD comprise a highly variable group of malformations affecting the heart, great vessels, and outflow tract ranging in severity and

Author for Correspondence: Jonathan T. Butcher, PhD, Assistant Professor, Department of Biomedical Engineering, 304 Weill Hall, Cornell University, Ithaca NY, 14853, Office: (607) 255-3575, Fax: (607) 255-7330, jtb47@cornell.edu.

The authors have no financial interests to disclose.

often times altering the hemodynamics in the heart. The ability to treat CHD and the survivability is varied. In many instances, minor septal defects do not require surgery (Roest and de Roos 2012) but complex malformations such as hypoplastic left heart syndrome require immediate postnatal surgical intervention and the survival rate after the first week of life for these patients can be as low as 39% (Samanek 1992). Within the past three decades, improvements in fetal cardiovascular imaginghas been instrumental in evaluating the heart and diagnosing CHD prenatally (Kleinman, Hobbins et al. 1980) contributing to the postnatal survival of patients born with complex CHD (Bonnet, Coltri et al. 1999; Tworetzky, McElhinney et al. 2001). Furthermore, when a CHD is present, evaluating the spatial progression of the defect over gestation allows for important developmental information to be learned (Hornberger, Sanders et al. 1995; Hornberger, Sanders et al. 1995). With the advancements in imaging technologies, surgical planning and intervention is improving but not all defects are detected prior to birth.

Beyond the heart, patients who suffer from a CHD have a higher susceptibility for further long term health concerns. Conditions such as hyponatremia, anemia, and renal dysfunction are frequently encountered along with a higher susceptibility for developing dementia in patients who have a CHD (Dimopoulos, Diller et al. 2008; Dimopoulos, Diller et al. 2009; Dimopoulos, Diller et al. 2010; Gorelick, Scuteri et al. 2011). Many of these long term complications are due to blood flow changes from the malformation, causing a cascade of events resulting in lifelong health problems. Prenatal assessment of CHD has the ability to improve perioperative management and surgical outcomes that can ideally return the hemodynamic environment of the heart close to its native state, reducing the downstream affects caused by systemic blood flow changes.

The genetic contribution to the development of a CHD varies with the malformation but less than 10% of many common defects can be traced to a genetic origin (Pierpont, Basson et al. 2007), suggesting that there are several other mechanisms at the root of CHD development paving the way for scientific research. Several imaging modalities that exist beyond the clinic allow scientists to visualize the dynamic and tortuous geometries seen through cardiogenesis revealing a mechanistic understanding of cardiovascular development. Understanding the functional contributions of multiple cell types, secreted factors, and mechanical influences in the developing heart is critical for identifying the origins of cardiac anomalies. Progression through the use of animal models has been made through surgical manipulations and genetic perturbations to dissect out contributions to proper cardiogenesis and dismorphogenesis. Scientists have made considerable strides in piecing together the complex mechanisms involved during cardiogenesis but many questions still remain.

Multi-dimensional, dynamic imaging is an invaluable contribution to the study of cardiovascular development, in particular heart development. Imaging systems available for the clinicis limited with ultrasound being the most widely used modality (Roest and de Roos 2012). Scientifically, several methods exist for imaging the embryonic heart. Each modality used scientifically has its own advantages and limitations associated with it including resolution, depth of field, soft tissue contrast, and cost. In this review, we introduce common imaging modalities used clinically and scientifically to assess heart development discussing the capabilities and limitations for each. We then focus on the clinical significance of the

current scientific research utilizing these modalities. We conclude by discussing the translational importance between the research performed in the laboratory and fetal cardiac imaging in the clinic.

2.0 Clinical Fetal Cardiac Imaging

The foremost widely used imaging modality for fetal cardiac imaging is ultrasound. Ultrasound imaging offers several imaging modes, each of which generates different information about the developing heart. Collectively, the capabilities of ultrasound allow for anatomical and physiological abnormalities to be identified over a broad range of fetal development.

2.1 M-Mode and Two- Dimensional Ultrasound

M-mode (motion mode) ultrasound generates 1-dimensional spatial information along the axis of the sound beam with high (kHZ) temporal resolution. The fixed transducer position produces a single beam transverse to the heart. M-mode is not able to distinguish if structures are translating or rotating off of the beam axis (Bushberg, Seibert et al. 2002). M-mode ultrasound imaging can evaluate motion of the heart such as the heart rate, valve function, and myocardium movements and is used to assess basic anatomical measurements such as wall thickness and chamber size (Rajiah, Mak et al. 2011).

More specifically, the heart rate and rhythm is evaluated above and below the atrioventricular valve through the atrial and ventricular walls (Allan 2004). Supraventriular tachycardia and atrial flutter, the most common fetal arrhythmias, are determined in this manner (Small and Copel 2004). Furthermore, M-mode ultrasound imaging can be used to measure the shortening fraction and the peak systolic and diastolic ventricular diameters (Rajiah, Mak et al. 2011). The shortening fraction represents the difference between the end diastolic and end systolic ventricular diameters normalized to the end diastolic ventricle diameter. This metric is indicative of ventricular function (2006).

Evaluation of the cardiac long axis function utilizes M-mode ultrasound imaging, specifically when analyzing annular displacement in the right ventricle due to the longitudinal orientation of the muscle (Allan 2004; Sklansky 2004). Gardiner and colleagues found that a near linear relationship exists between maturation of the fetus and long axis function within the heart using M-mode ultrasound imaging (Gardiner, Pasquini et al. 2006). The metrics that Gardiner established provide baseline information for long axis function that can be used to evaluate the health and function of the heart throughout gestation using long axis assessments. Long axis abnormalities can be detected much earlier in development through M-mode ultrasound and are indicative of ischemia from changes in wall stress and abnormal coronary perfusion seen in the earlier stages of a diseased heart (Gardiner, Pasquini et al. 2006).

Two-dimensional (2D, B-Mode) ultrasound has been the established clinical method for fetal heart imaging for the past 20 years (Sklansky 2004). 2D ultrasound transducers have high spatial and temporal resolution providing valuable diagnostic information but it is largely dependent on the expertise of the ultrasound technician. 2D ultrasound images are

comprised of a set of 2D slices through the tissue but proper interpretation of the results requires mental acuity to visualize the information in three dimensional space (Stoll, Alembik et al. 1998; Allan 2000).

2.2 Three-Dimensional and Four-Dimensional Ultrasound

Three-dimensional (3D) ultrasound acquires projections through multiple angles of the fetus and then the image is reconstructed into a three dimensional volume in a similar manner how a CT scan is acquired. 3D imaging allows for quantitative spatial metrics to be determined and multiple planes to be viewed revealing complicated geometry that is not easily viewed on traditional 2D scans (Rajiah, Mak et al. 2011). Furthermore, four-dimensional (4D) imaging or real time 3D imaging incorporates temporal resolution coupled with cardiac gating for viewing the fetus in time and three spatial dimensions.

Within the last 15 years, research in fetal cardiac imaging using 3D/4D ultrasound has increased with prominent studies being reported since the mid-1990s (Deng, Gardener et al. 1996; Nelson, Pretorius et al. 1996; Sklansky, Nelson et al. 1999; Meyer-Wittkopf, Cooper et al. 2001; Deng, Yates et al. 2002; Maulik, Nanda et al. 2003). The primary objective of 3D ultrasound has been to acquire a volumetric dataset for reconstruction of the fetal heart in three spatial dimensions. In more recent years, studies have focused on improved processing and identification of cardiac fetal abnormalities for better diagnostic capabilities. Modifications to the ultrasound transducer are one method used to improve ultrasound imaging. For example, a transducer using matrix technology acquires a pyramid-shaped data set simultaneously minimizing motion artifacts that affect the reconstructed data set in post-processing (Herberg, Steinweg et al. 2011). Herberg and colleagues assessed the ability of fetal 3D reconstructive echocardiography using a free hand technique and matrix technology to compare fetal cardiac findings as compared to the traditional 2D ultrasound. The visualization rate of real time 3D echocardiography using matrix technology was equivalent to 2D ultrasound and significantly lower for free hand reconstruction (Herberg, Steinweg et al. 2011). Real-time 3D ultrasound images were acquired in the four chamber view and left ventricular outflow tract view (Figure 1) (Herberg, Steinweg et al. 2011). Real time 3D echocardiography improved visualization of the short axis, aortic arch, and ductal arch over the 2D ultrasound standard (Herberg, Steinweg et al. 2011). When compared to postnatal findings, real time 3D and 2D ultrasound was significantly more accurate than free hand 3D ultrasound echocardiography (Herberg, Steinweg et al. 2011). Furthermore, Zabadneh and colleagues determined that 3D ultrasound can serve as a complete diagnostic for congenital heart defects (Zabadneh, Santagati et al. 2011). 3D ultrasound provides information on extracardiac malformations commonly seen with congenital heart disease providing a complete diagnosis of the syndrome (Zabadneh, Santagati et al. 2011). The diagnostic accuracy for congenital heart defects using 3D ultrasound was superior with optimal results found in fetuses older than 24 weeks, where heart morphology was best viewed (Zabadneh, Santagati et al. 2011).

Fetal cardiac ultrasound imaging employs a four chamber view for diagnosing intracardiac CHD (Allan, Crawford et al. 1986; Copel, Pilu et al. 1987; Chaoui 2003). Conotruncal abnormalities may not be visualized with this method (2006). Anomalies in the ductal and

aortic arches can be imaged with the three vessels and trachea (3VT) view to improve the detection of CHD (Yagel, Arbel et al. 2002). Moreover, live xPlane imaging is an acquisition technique using a matrix-array probe which enables visualization of the fetal heart pulsations in real time (Maulik, Nanda et al. 2003; Acar, Dulac et al. 2005; Goncalves, Espinoza et al. 2006). Two real-time, high resolution views can be displayed simultaneous with live xPlane imaging. A study by Xiong and colleagues demonstrated that starting with the four chamber view plane, several additional visualization planes are easily found including the left outflow tract, right outflow tract, and 3VT (Xiong, Chen et al. 2012). In a simultaneous study, Xiong and colleagues established a method to use 3D ultrasound coupled with live xPlane imaging to visualize the ductal and aortic arches from the 3VT view simultaneously (Xiong, Chen et al. 2012). Xiong et al found that the 3VT view with live xPlane imaging detected CHD not easily seen with the standard 4 chamber view (Xiong, Chen et al. 2012). The accuracy of the clinical measurements was confirmed through either autopsy following pregnancy termination or postnatal echocardiography (Xiong, Chen et al. 2012). In an additional study, Xiong and colleagues used 3D ultrasound with live xPlane imaging to view a ventricular septal defect in a fetal patient (Figure 1) (Xiong, Liu et al. 2012).

Multidimensional, dynamic imaging extends to flow imaging techniques for further assessment of the fetal heart. Classically, Doppler principles has been used for blood flow imaging where differences in the blood velocity is resolved in space but with a resolution trade-off as compared to 2D ultrasound imaging techniques (Bushberg, Seibert et al. 2002). B-flow imaging is a technique that provides direct visualization of blood flow with gray-scale sonography (Furuse, Maru et al. 2001). B-flow imaging is a non-Doppler founded technology that utilizes digital ultrasound to display flow based on intravascular echoes in real time (Wu, Zhang et al. 2012). Wu and colleagues determined through a clinical study that real time 3D ultrasound with B-flow imaging detected the outflow tracts, great arteries, and veins that merge into the heart in fetuses with cardiac anomalies establishing a method which aides in the evaluation of fetal cardiovascular hemodynamics (Wu, Zhang et al. 2012).

2.3 Image Processing and Analysis

2.3.1 Volumetric Reconstruction—A direct volume scan is obtained when the scan time of the ultrasound is significantly less than the spatial movement of the anatomy being imaged; therefore, the movement of the fetal anatomy is negligible (Deng and Rodeck 2004). Prominent phasic changes in the fetal heart include filling and ejection of the ventricles. These volume changes occur in 50 to 100ms; therefore, a minimum of 50ms/volume is required for acquisition using a direct volume scan (Deng and Rodeck 2004). Wang et al have shown that this minimal requirement can be met with real time 3D ultrasound imaging using a 2D array transducer (Wang, Deng et al. 2003).

In contrast, an indirect volume scan uses a set of slices containing data of the fetal heart from a cross sectional transducer. In post processing, the slices are computationally binned based on time points within the cardiac cycle and then 3D volumes are ascertained (Deng and Rodeck 2004). Using an indirect method for obtaining volumetric information is the

most widely used method clinically due to the high spatial and temporal resolution of the transducer. Research has used spatial tracking (Nelson 1998) and temporal tracking (Deng, Gardener et al. 1996; Nelson, Pretorius et al. 1996; Deng, Birkett et al. 2001) for obtaining the data set.

2.3.2 Image Gating—Specification of image acquisition, referred to as gating, is designed to limit motion artifacts either during the image scan (prospective) or computationally after the entire dataset has been obtained (retrospective) (Gregg and Butcher 2012). Prospective gating requires laborious upfront instrumentation for synchronizing the image acquisition with the fetal cardiac cycle but the back end computation is minimal. Conversely, retrospective gating acquires all possible images within the dataset and then image slices are coupled through spatial or temporal correlation. As previously mentioned, indirect volumetric scans use retrospective gating techniques to reproduce the fetal heart volumes computationally based on phase information after the scan is complete.

2.3.3 Multi-Planar Reformatting and Surface Displays—Due to the variability in ultrasound acquisition attributed to the experience of the technician, scan time, and fetal position, mutli-planar reformatting corrects for variability in image acquisition by re-establishing the plane being viewed from variations in the dataset. Mutli-planar reformatting did not become possible until 3D ultrasound (Sklansky, Nelson et al. 1997). Direct acquisition of the desired fetal cardiac view is preferable where an experienced operator can direct the sound beam towards the specific anatomy needed to be imaged (Deng and Rodeck 2004).

Furthermore, the ability to change the surface characteristics computationally of the cardiac anatomy enables easier quantification of anatomical metrics. This is applicable in instances where the cardiac chambers are displayed as solid objects, known as a negative surface display (Deng and Rodeck 2004). Volumetric analysis of the fetal heart chambers over the course of development becomes increasingly clear with negative surface displays. Color surface displays have been useful with 3D/4D blood flow ultrasound imaging. Blood flow directionality information is discerned effectively with color surface displays seen in a study by Deng and colleagues (Deng, Yates et al. 2002).

2.3.4 Spatiotemporal Image Correlation—Spatiotemporal image correlation (STIC) reconstructs a volumetric dataset within an entire cardiac cycle based on a 3D dataset from approximately 1500 B-mode images slices from five transverse planes acquired during the imaging scan (Godfrey, Messing et al. 2012). STIC processing coupled with 3D/4D ultrasound has emerged as a powerful diagnostic tool for assessing the fetal heart and has the ability to increase diagnostic accuracy of CHD (DeVore, Falkensammer et al. 2003). In post-processing, systolic peaks are identified and the fetal heart rate is back calculated (Figure 2)(Yagel, Cohen et al. 2007). STIC provides high levels of information which can counteract the ambiguities associated with fetal imaging concerning the fetal placement during the scan and the ultrasound technician. Adriaanse and colleagues conducted a 3 year study that examined the diagnostic agreement of multiple physicians for CHD screenings through a telemedicine approach using 4D ultrasound with STIC. Through a telemedicine setting, cardiac abnormalities can be accurately diagnosed by a medical expert and

agreement amongst medical professionals based on the 4D ultrasound with STIC (Adriaanse, Tromp et al. 2012). Coupled with 3D/4D ultrasound STIC has the capability to address ambiguities seen in the clinic but also provides adequate information for telemedicine settings which become increasingly desirable for rural communities who do not have access to echocardiographic specialists. The most problematic limitation of STIC is motion artifacts from fetal breathing which distorts the B-mode 2D image stack leading to inaccuracies in the volume rendering (Yagel, Cohen et al. 2007). In an exam, the quality of the B-mode images is assessed prior to accepting the volumetric information that is given through STIC processing (Yagel, Cohen et al. 2007).

2.4 Future Directions

For the improvement of fetal cardiac imaging, spatial resolution and depth of field parameters have to be optimized. For detecting cardiac malformations in early development, high resolution ultrasound imaging is needed to resolve the small, tortuous anatomy. Ultrasound biomicroscopy offers resolution capabilities in the microscopic range (Deng and Rodeck 2004) but the depth of penetration is not sufficient for imaging through the mother to the fetus, limiting this technology to scientific inquiry to date. Studies are exploring the use of magnetic resonance imaging for fetal cardiac assessment. Votino and colleagues imaged 106 fetuses, 66 that were normal and 40 which had a CHD using magnetic resonance imaging. The four chamber view of the heart was visualized in 98.1% of the cases and the sensitivity for detecting a malformation was 88% with a specificity of 96% (Votino, Jani et al. 2012). Imaging the right and left outflow tract was influenced by fetal movement and the sensitivity for detecting a cardiac defect of the right and left outflow tracts was 59% and 63% respectively (Votino, Jani et al. 2012). Votino et al concluded that magnetic resonance imaging was sufficient for detecting heart anomalies in the four chamber view but not reliable for the outflow tract malformations and could be used as a secondary method for assessing the heart with ultrasound still being the gold standard (Votino, Jani et al. 2012). Minimally invasive approaches for diagnosis, monitoring, and prenatal intervention are attractive for endoscopic ultrasound applications with studies becoming prominent a little over a decade ago (Sydorak, Nijagal et al. 2001). More recently, prenatal intervention is suggested for the most severe of CHD where postnatal survival is low. In the case of hypoplastic left heart syndrome, surgical interventions are attractive given the bleak outcome postnatal. Two groups have explored balloon valvuloplasty for aortic valve stenosis seen in these cases (McElhinney, Marshall et al. 2009; Arzt, Wertaschnigg et al. 2011). Technical success is high for this procedure but several peri-operative complications exist including critical bradycardia, thrombosis, and fetal demise (Arzt and Tulzer 2011). The success rate of complex prenatal interventions is low and many improvements still remain. The clinical ideal for prenatal intervention is having a multi-modal, multifunctional catheter which has optical and ultrasound imaging capabilities coupled with surgical features (Deng and Rodeck 2004) but the design of these devices plus the technical parameters of prenatal surgery provide areas for impactful research.

3.0 Scientific Embryonic Cardiovascular Imaging

Growth, patterning, and differentiation during embryogenesis occur within multiple length and time scales (Dehaan and Ebert 1964). Exploring the functional contributions influencing morphogenesis has been aided by the use of animal models and a variety of assays to analyze these contributions in vitro, in situ, and in vivo. Genetic mutations and microsurgical interventions have slowly but consistently elucidated mechanisms implicated in tissue morphogenesis and dysmorphogenesis. Reporter models and local labeling strategies have been effective to identify and follow heterogeneous tissue patterning and fate decisions during embryonic development. Advancing imaging technology, in parallel with experimental improvements, is critical for identifying developmental phenomena and following downstream effects. Direct microscopic visualization of tissues using optical technologies has been the longstanding imaging method of choice for the earliest stages of development but it lacks the depth of penetration needed for late stage embryonic studies when the tissues have become dense and light scattering. Dynamic and inherently three dimensional imaging technologies possess the high spatial and temporal resolution required to capture cardiac development from early to late stages. In the case of scientific research, the modalities most widely used are ultrasound, optical coherence tomography (OCT), micro-computed tomography (microCT), and magnetic resonance imaging (MRI). Each technology has differences in capabilities with rational trade-offs that need to be considered for each experimental situation.

3.1 Imaging Technology Overview and Comparisons

Ultrasound imaging uses short pulses of high frequency sound waves that scatter when transmitted and/or reflected though tissue based on the individual material properties inherent to the anatomy being imaged. The spatial resolution is defined as half the pulse length; therefore, high frequency transducers result in an increase in spatial resolution but this is in trade-off with the depth of field and amount of scatter (Lieu 2010). Ultrasound biomicroscopy enables the earliest embryonic stages to be visualized by using uncharacteristically high probe frequencies (30–50MHz) not available clinically (Srinivasan, Baldwin et al. 1998; Phoon, Aristizabal et al. 2000; Foster, Zhang et al. 2002; Zhou, Foster et al. 2002; Zhou, Foster et al. 2003; Phoon, Ji et al. 2004). Embryonic phenotyping with ultrasound has shown the developing of the atrioventricular canals transiently in the chick (Figure 3)(Butcher, McQuinn et al. 2007). For embryonic heart imaging, axial resolution capabilities have been reported at 30μm (Ji and Phoon 2005). Ultrasound biomicroscopy coupled with Doppler flow imaging has been used to assess the cardiovascular hemodynamics for over the past decade (Christopher, Burns et al. 1996; Christopher, Burns et al. 1997).

The basic technology of OCT functions on a similar principle as ultrasound but light is used as the signal source versus sound. An interferometer is used to interrogate reflected light from a sample at a given depth. OCT has a depth of penetration of approximately 3mm and is capable of producing 3D and 4D data sets (Liu, Wang et al. 2009). Using an array or sweeping the optical source, OCT has improved signal-to-noise ratio (SNR) compared to imaging without these techniques which can result in low signal strength from multiple

sources of reflectance, much like the obstacles associated with ultrasound imaging. Scan rates as fast as 100 2D frames/second and 5 3D volumes/second have been reported, yielding some of the fastest multi-dimensional acquisition rates achievable (Luo, Marks et al. 2006). Dynamic morphology studies using OCT have gained traction recently in developmental biology. Specifically, early heart looping and contractions have been measured in the first stages of cardiogenesis (Manner, Thrane et al. 2009) and later stage kinematics was measured in the embryonic (Figure 4) heart (Luo, Marks et al. 2006). Doppler technology implemented with OCT has been used to quantify hemodynamic profiles in the heart using particle image velocimetry scatter tracking algorithms (Jenkins, Peterson et al. 2010; S, D et al. 2011).

For the past 15 years, microCT has been used experimentally to quantify complex anatomy with high spatial resolutions based on the attenuation of x-rays through the tissue (Butcher, Sedmera et al. 2007). In experimental research, a microCT image is obtained by the attenuation of x-rays through the sample detected by a gamma camera opposite of the x-ray emitter on the gantry of the machine. The image is reconstructed through back projection based on the 360° discrete measurements taken around the sample and then fully registered into a three dimensional stack of planar slices (Butcher, Sedmera et al. 2007).

The resolution capabilities of microCT are superior and the time for image acquisition is unmatched but the attenuation of x-rays through soft tissue is poor. For fixed embryonic studies, several iodine and high atomic weight molecule based exogenous soft tissue contrast has been used to combat this short coming. Osmium tetroxide has long been considered a gold standard for microCT imaging in embryos providing high levels of soft tissue contrast and clear tissue boundaries but it is most optimal for earlier and mid stages of development (Johnson, Hansen et al. 2006; Litzlbauer, Neuhaeuser et al. 2006; Bentley, Jorgensen et al. 2007; Zhu, Bentley et al. 2007)(Faraj, Cuijpers et al. 2009; Metscher 2009; Kim, Min et al. 2011). Lugol's solution, iodine potassium iodide, gallocyanin-chromalum, and phosphotungstic acid stains are addition commonly used exogenous soft tissue contrast for microCT (Bentley, Jorgensen et al. 2007; Metscher 2009; Degenhardt, Wright et al. 2010; Kim, Min et al. 2011). Using osmium tetroxide, Kim and colleagues imaged chick embryos at 25μm to segment and quantify the cardiac chambers of the developing heart from day 4 to day 10 of development (Figure 5) (Kim, Min et al. 2011). Butcher and colleagues perfused chick embryos with Microfil (Flow Tech, Inc) a radiopaque polymer that fills the luminal spaces of the embryonic heart (Butcher, Sedmera et al. 2007). Based on the microCT heart images from chicks ranging in age from Hamburger and Hamilton stages 17–30, the multi-step looping and septation of the heart is easily viewed from the image surface renderings. Resolution capabilities for microCT has been reported to be less than 10μm (Guldberg, Ballock et al. 2003) and in some cases in the resolution range of hundreds of nanometers where cell populations can be discerned, but with much more limited fields of view (Metscher 2009). For live imaging, spatial resolution of 25μm is achievable (Kim, Min et al. 2011) with scan times as little as two minutes for 50μm resolution (Henning, Jiang et al. 2011).

MRI capitalizes on the inherent magnetic properties of tissues based on the variations in water content. Frequency and phase information for each image slice is stored and

represented as a stack of two dimensional slices which is interpolated as a three dimensional volume. The exogenous soft tissue contrast capability of MRI is superior, but the image acquisition rate is long for embryonic studies (6–24hr), presenting non-trivial challenges for live embryonic imaging (Turnbull and Mori 2007). Although spatial resolutions of 10μm voxel size are achievable, resolution is often made much coarser (hundreds of microns) and with skewed elements to balance SNR with reasonable scanning time. MRI contrast can be further enhanced with gadolinium chelates and super paramagnetic iron oxide particles, which can also be incorporated into labeling strategies for molecular targeting and imaging evolution of cell populations (Liu and Frank 2009). Multiple embryos can be placed in the scanner at one time, all fixed and inserted into a standard mouse head imaging coil. Higher magnetic field strength is a consideration for improving the image quality, in some embryonic studies 11.7 T and 9.4T has been used over or in conjunction with the 7T (Schneider, Bamforth et al. 2003; Petiet, Kaufman et al. 2008). Additionally, with using fast spoiled three dimensional gradient echo sequences with T1 weighting, asymmetric sampling and/or an expanded range, shorter scan times have been achieved for mouse embryos (Schneider, Bamforth et al. 2003; Petiet, Kaufman et al. 2008). Petiet and colleagues used MRI to produce high resolution images of fixed, embryonic mice through development and into the first postnatal days (Figure 6) (Petiet, Kaufman et al. 2008)

A comparative summary of the advantages and limitations of ultrasound, OCT, microCT, and MRI are given in Table 1. The resolution capabilities are largely similar with each modality, but incur significant differences in depth of field, cost, and scan times. Ultrasound is inherently real time and allows for a short scan and the overall cost is less than microCT and MRI. OCT costs the least with high spatial resolution capabilities but the depth of field is lacking compared to microCT and MRI. MicroCT has a high upfront cost as compared to ultrasound and OCT but this is compensated for in the high depth of field and resolution capabilities of the machine within a reasonable scanning time. MRI produces the highest level of soft tissue contrast without the need of exogenous agents but the scan times are significantly longer, especially at high resolutions. Resolution demands limit the depth of view, which overall limits its broad applicability for visualizing embryonic morphogenesis.

3.2 Clinically Relevant Animal Models in Cardiogenesis Research

As human imaging is largely restricted to post cardiac morphogenesis, animal models are relied upon to inform our understanding, in particular dynamic behaviors. The most commonly used four chambered embryonic models are avian and murine. Avian models (chick and quail) are inexpensive and the embryo is easily accessed by either an ex ovo culture or through windowing the egg shell in an in ovo egg culture. Avian models however have limited molecular targets for tissue specific studies and have not been widely manipulated genetically (Chapman, Lawson et al. 2005; Bower, Sato et al. 2011; Seidl, Sanchez et al. 2013). Surgical perturbations of avian embryos, achieved via a metallic clip or ligation, enable quantitative understanding of the role of hemodynamic forces on heart development (Broekhuizen, Hogers et al. 1999; Ursem, Struijk et al. 2001; Ursem, de Vos et al. 2002; Stekelenburg-de Vos, Ursem et al. 2003; Stekelenburg-De Vos, Steendijk et al. 2005; Stekelenburg-de Vos, Steendijk et al. 2007; Oosterbaan, Ursem et al. 2009). Kowalski and colleagues have recently combined OCT imaging with computational analysis to

examine the hemodyamic environments within the developing aortic arches of chicks (Kowalski, Dur et al. 2013). Chick embryos have been imaged with microCT in fixed and live studies. With the high spatial resolution of microCT, Kim and colleagues generated mathematical relationships for volumetric growth of major organ system including the heart (Kim, Min et al. 2011). Using a navigated retrospective gating protocol, Holmes et al determined the cardiac and respiratory cycles of chick embryos (Holmes, McCabe et al. 2008). The method established by Holmes has to potential for multi-slice imaging, serial imaging of the chick heart longitudinally through cardiogenesis (Holmes, McCabe et al. 2008). Hogers and colleagues have imaged live quail embryos with induced cardiac malformations from clipping the right lateral vitelline vien (Hogers, van der Weerd et al. 2009). Hogers et al obtained high quality MRI images of quails ranging from days 3–11 of development with a spatial resolution of 78–90μm with image slices ranging from 300–500μm (Figure 6)(Hogers, van der Weerd et al. 2009).

The murine animal model is much more easy to genetically manipulate than the chick and its use has contributed much to our understanding of the molecular networks regulating cardiogenesis. Murine embryos are smaller however and require in utero growth, significantly limiting opportunities for surgical and/or biomechanical perturbation. Ultrasound biomicroscopy has been applied to murine embryos as early as E5.5, and the cardiovascular system imaged at E8.25 with 30μm resolution (Ji and Phoon 2005). Ultrasound biomicroscopy coupled with Doppler flow imaging for evaluation of cardiac hemodynamics has been used for guided flow measurement of normal and genetically altered live mouse embryos (Christopher, Burns et al. 1996; Christopher, Burns et al. 1997; Aristizabal, Christopher et al. 1998; Le Floc'h, Cherin et al. 2004; Ji and Phoon 2005). Using unenhanced (Dhenain, Ruffins et al. 2001; Schneider, Bamforth et al. 2003; Bamforth, Braganca et al. 2004) and gadolinium enhanced (Huang, Wessels et al. 1998) imaging, the cardiovascular system in fixed murine embryos has been completed with MRI. By imaging multiple preserved embryos simultaneously (up to 32), the burden of long scan times can be decreased, also enabling higher throughput for phenotyping (Turnbull and Mori 2007). For live murine studies, non-periodic bulk rotations of the embryos and possibly the mother require long scan times and more intensive post-processing for subtracting out the motion artifacts (Nieman, Szulc et al. 2009).

A comparative analysis of avian and murine cardiac development events to the equivalent gestation period in humans is given in Table 2. Outlined in the table are the first cardiac events described in days for human development, embryonic days for mouse development and is the Hamburger and Hamilton (HH) (Hamburger and Hamilton 1951) indexing system for the chick development.

3.3 Image Processing

Quantitatively visualizing the highly dynamic processes in embryonic development requires obtaining high quality images devoid of motion artifacts. This can be achieved either through post-acquisition processing or from prospective gating of image acquisition. In embryonic studies, gating with the heart has been achieved through following the non-symmetric myocardial cross section movement for each imaging plane during the cardiac

cycle (Liebling, Forouhar et al. 2005). Using OCT data, Liu and colleagues derived spatially and temporally unique line scans to render 4D information of the avian outflow tract (Liu, Wang et al. 2009; Liu, Wang et al. 2009). Yoo et al translated the optical probe in OCT image acquisition to generate spatiotemporal overlapping fields of view that were re-synchronized yielding a 6 fold increase in imaging frame rate in the embryonic rat heart (Yoo, Larina et al. 2011). Once images containing relevant information are acquired, image restoration seeks to improve feature detection and image contrast through deconvolution and registration (Gregg and Butcher 2012). Image analysis is the means by which the information contained in each image voxel is translated into digital information that can be measured or compared. From this information, computational models, simulations, and estimations of functional parameters can be ascertained which would otherwise be difficult if not impossible to measure directly (Gregg and Butcher 2012).

4.0 Translational Impact and Opportunities in Cardiogenesis Imaging Research

Dynamic changes in cardiac morphogenetics likely conceal much of the unknown frontiers in embryonic development, in particular for cardiovascular development. Quantitative, multi-dimensional imaging technologies will only increase in value for identifying and following causes and consequences of genetic, surgical, and microenvironmental perturbations.

Genetic mutations are known to play a role in cardiac malformation development, with the highest prevalence of genetic associated CHD linked with other abnormalities (Pierpont et al 2007). Studying animal models with genetic associated malformations provides information about the propagation of these anomalies throughout development. For example, mutant embryonic mouse lines known to have right ventricle malformations have been studied using a 7T MRI magnet with gadolinium-based contrast agent mixed with 7% gelatin (Wadghiri, Schneider et al. 2007). Disrupting the mechanical environment in the embryo through surgical interventions and modeling strategies has lead to many studies considering the biomechanical influences affecting cardiovascular development. KeremPekkan and colleagues have completed multiple studies examining the effects of hemodynamic loading and aortic arch development in the chick embryo through in vivo studies and computational simulation. Assessing in vivo arch morphology with fluorescent dye and vascular based growth models, the Pekkan group found that the outflow tract orientation is dynamic during morphogenesis, changing the hemodynamic load through the aortic arches which has a significant influence on downstream patterning events where congenital anomalies can arise (Kowalski, Teslovich et al. 2012). Furthermore, using microinjected dye recordings coupled with high resolution OCT, Kowalski, Pekkan et al quantified the patterns and aortic arch anatomy which was then used for computational fluid dynamic analyses to measure flow and wall shear stress (WSS) (Figure 7)(Kowalski, Dur et al. 2013). They found that small increases in WSS are followed by vascular remodeling meant to combat the changes in loading, possibly impacting the cardiac events and giving opportunity for aberrant morphology to arise (Kowalski et al 2013). Based on Doppler ultrasound imaging flow profiles and three dimensional anatomical information from microCT images, Yalcin and

colleagues characterized the hemodynamic environment of the atrioventricular canal in the chick embryo from HH17-HH30 through the development and optimization of a computational fluid dynamic model that matched in vivo observations (Figure 7)(Yalcin, Shekhar et al. 2011). Yalcin et al established a baseline to support future hemodynamic investigations through characterizing the WSS and fluid flow patterns.

In addition to viewing and quantifying, imaging technology can also be used to intervene in development through perturbing normal tissue patterning. Focused femtosecond laser photoablation has been achieved in the atrioventricular canal of embryonic chicks (Yalcin, Shekhar et al. 2010). Photoablation can occlude defined areas of the developing heart while keeping the surrounding tissue intact. These small perturbations, coupled with hemodynamic analysis, enables unique information about the local hemodynamic environments in the embryo and their global affects on development. The generation of these diseased animal models has emerged as a new, in vivo tool for studying cardiogenesis. Ultrasound has been shown to noninvasively alter development. Histotripsy is a technology that uses focused ultrasound to generate cardiac defect models. It has been used to create atrial septal defects in a canine model (Xu, Owens et al. 2010) and lesions within fetal sheep (Kim, Min et al. 2011). Taking advantage of this technology is particularly attractive for more in depth embryonic studies.

One of the greatest challenges for embryonic imaging studies is achieving appropriate levels of soft tissue contrast in the image allowing for tissue quantification. MRI has endogeneous soft tissue contrast based on the technology itself and there are options for gadolinium based agents as well. For imaging the developing heart with microCT, using an iodinated or high atomic weight agent is required for producing quality images but almost all microCT contrast agents are embryotoxic, limiting studies to fixed specimens. Efforts are being focused on the development of non-toxic exogenous contrast for live experiments. Henning et al established the first live in vivo embryonic avian study with microCT using Visipaque™ (iodixinol-VP), an iodine based contrast agent produced by General Electric that was found to be non-toxic for the chick embryo. VP produced 1060HU of contrast at 50μm resolution and x-ray radiation up to 798 mGray did not produce morphological defects through the first 10 days of development, encompassing all of cardiogenesis (Henning, Jiang et al. 2011). Henning and colleagues characterized VP for embryonic imaging in the avian embryo including biodistribution and volumetric quantification studies of the heart from day 3 to day 10 of development (Henning, Jiang et al. 2011). Exogenous contrast standards for imaging clear embryos quickly based on their small molecular sizes. Recent developments suggest that nanoparticle based contrast agents could be appropriate in embryos for prolonging the residence time and biodistribution properties (Gratton, Pohlhaus et al. 2007). Significant efforts are in progress for producing highly reflective contrast agents for OCT, mainly in the form of polystyrene microspheres and pyrolle nanoparticles (Boppart, Oldenburg et al. 2005; Filas, Varner et al. 2011).

Environmental control of the embryonic animal model system is important for maintaining consistency and true physiologic conditions for the study. Without environment control, animal heart rates can fluctuate and arrhythmias may occur. Reducing scanning times and maintaining standard physiologic temperature and humidity is imperative for live imaging

studies. Different environmental control chambers have been designed for imaging. Henning and colleagues designed an environment control chamber which maintains temperature at approximately 37°C and 55% humidity (Henning, Jiang et al. 2011). Additional factors being considered for live embryonic imaging is the movement of the embryo. One method for limiting embryonic movement is to cool the embryo prior to imaging. Hogers and colleagues cooled quail embryos to 4°C for one hour prior to a MRI scan (Hogers, van der Weerd et al. 2009). There is a possibility that cooling the embryo may induce adverse effects with the cardiovascular system. Pharmacological intervention is another possibility with agents that temporarily paralyze skeletal muscle without affecting the heart.

Capitalizing on dynamic and multi-dimensional imaging technologies for viewing, quantifying, and perturbing embryonic development presents a plethora of opportunity for exploring new realms of cardiovascular development not easier studied prior to these innovations but more clinically motivated, it allows for the origins of CHD to be investigated. Understanding the beginnings of CHD and how they evolve over cardiogenesis is critical for engineering strategies to better diagnose these malformations prenatally and inspiring new technologies for treating them either pre or postnatally. Given the poor outcome of severe CHD and the long term care required for many cardiac malformations, knowing the progression of CHD in utero and having appropriate metrics to understand them by can only benefit the patient and the overall treatment. Embryonic studies support this effort through uncovering genetic, mechanical and biochemical influences that guide the complexities in heart development.

Acknowledgements

This research was supported in part by grants from the National Science Foundation (CBET #0955172 to JTB) and a GDRS (to CG), and the National Institutes of Health (HL110328).

References

1. Cardiac screening examination of the fetus: guidelines for performing the 'basic' and 'extended basic' cardiac scan. Ultrasound in Obstetrics & Gynecology. 2006; 27(1):107–113. [PubMed: 16374757]
2. Acar P, Dulac Y, et al. Real-time three-dimensional fetal echocardiography using matrix probe. Prenatal Diagnosis. 2005; 25(5):370–375. [PubMed: 15906427]
3. Adriaanse BME, Tromp CHN, et al. Interobserver agreement in detailed prenatal diagnosis of congenital heart disease by telemedicine using four-dimensional ultrasound with spatiotemporal image correlation. Ultrasound in Obstetrics & Gynecology. 2012; 39(2):203–209. [PubMed: 21611994]
4. Allan L. Congenital heart disease - Antenatal diagnosis of heart disease. Heart. 2000; 83(3):367–370. [PubMed: 10677423]
5. Allan L. Technique of fetal echocardiography. Pediatric Cardiology. 2004; 25(3):223–233. [PubMed: 15360115]
6. Allan LD, Crawford DC, et al. PRENATAL SCREENING FOR CONGENITAL HEART-DISEASE. British Medical Journal. 1986; 292(6537):1717–1719. [PubMed: 3089369]
7. Aristizabal O, Christopher DA, et al. 40-MHz echocardiography scanner for cardiovascular assessment of mouse embryos. Ultrasound in Medicine and Biology. 1998; 24(9):1407–1417. [PubMed: 10385963]
8. Arzt W, Tulzer G. Fetal surgery for cardiac lesions. Prenatal Diagnosis. 2011; 31(7):695–698. [PubMed: 21671460]

9. Arzt W, Wertaschnigg D, et al. Intrauterine aortic valvuloplasty in fetuses with critical aortic stenosis: experience and results of 24 procedures. Ultrasound in Obstetrics & Gynecology. 2011; 37(6):689–695. [PubMed: 21229549]
10. Bamforth SD, Braganca J, et al. Cited2 controls left-right patterning and heart development through a Nodal-Pitx2c pathway. Nature Genetics. 2004; 36(11):1189–1196. [PubMed: 15475956]
11. Bentley MD, Jorgensen SM, et al. Visualization of three-dimensional nephron structure with microcomputed tomography. Anatomical Record-Advances in Integrative Anatomy and Evolutionary Biology. 2007; 290(3):277–283.
12. Bonnet D, Coltri A, et al. Detection of transposition of the great arteries in fetuses reduces neonatal morbidity and mortality. Circulation. 1999; 99(7):916–918. [PubMed: 10027815]
13. Boppart SA, Oldenburg AL, et al. Optical probes and techniques for molecular contrast enhancement in coherence imaging. Journal of Biomedical Optics. 2005; 10(4)
14. Bower DV, Sato Y, et al. Dynamic Lineage Analysis of Embryonic Morphogenesis Using Transgenic Quail and 4D Multispectral Imaging. Genesis. 2011; 49(7):619–643. [PubMed: 21509927]
15. Broekhuizen MLA, Hogers B, et al. Altered hemodynamics in chick embryos after extraembryonic venous obstruction. Ultrasound in Obstetrics & Gynecology. 1999; 13(6):437–445. [PubMed: 10423809]
16. Bushberg, JT.; Seibert, JA., et al. The Essential Physics of Medical Imaging. Philadelphia, PA: Lippincott Williams & Wilkins; 2002. Ultrasound; p. 469-553.
17. Butcher JT, McQuinn TC, et al. Transitions in early embryonic atrioventricular valvular function correspond with changes in cushion biomechanics that are predictable by tissue composition. Circulation Research. 2007; 100(10):1503–1511. [PubMed: 17478728]
18. Butcher JT, Sedmera D, et al. Quantitative volumetric analysis of cardiac morphogenesis assessed through mirco-computed tomograpy. Developmental Dynamics. 2007; 236(3):802–809. [PubMed: 17013892]
19. Chaoui R. The four-chamber view: four reasons why it seems to fail in screening for cardiac abnormalities and suggestions to improve detection rate. Ultrasound in Obstetrics & Gynecology. 2003; 22(1):3–10. [PubMed: 12858294]
20. Chapman SC, Lawson A, et al. Ubiquitous GFP expression in transgenic chickens using a lentiviral vector. Development. 2005; 132(5):935–940. [PubMed: 15673573]
21. Christopher DA, Burns PN, et al. A high-frequency continuous-wave Doppler ultrasound system for the detection of blood flow in the microcirculation. Ultrasound in Medicine and Biology. 1996; 22(9):1191–1203. [PubMed: 9123644]
22. Christopher DA, Burns PN, et al. A high-frequency pulsed-wave doppler ultrasound system for the detection and imaging of blood flow in the microcirculation. Ultrasound in Medicine and Biology. 1997; 23(7):997–1015. [PubMed: 9330444]
23. Copel JA, Pilu G, et al. FETAL ECHOCARDIOGRAPHIC SCREENING FOR CONGENITAL HEART-DISEASE - THE IMPORTANCE OF THE 4-CHAMBER VIEW. American Journal of Obstetrics and Gynecology. 1987; 157(3):648–655. [PubMed: 3631166]
24. Degenhardt K, Wright AC, et al. Rapid 3D Phenotyping of Cardiovascular Development in Mouse Embryos by Micro-CT With Iodine Staining. Circulation-Cardiovascular Imaging. 2010; 3(3): 314–U138. [PubMed: 20190279]
25. Dehaan RL, Ebert JD. MORPHOGENESIS. Annual Review of Physiology. 1964; 26:15-&.
26. Deng J, Birkett A, et al. Conversion of Umbilical Arterial Doppler Waveforms to Cardiac Cycle Triggering Signals: A Preparatory Study for Onlne Motion-Gated Three Dimensional Fetal Echocardiography. Ultrasound in Medicine and Biology. 2001; 27(1)
27. Deng J, Gardener JE, et al. Fetal echocardiography in three and four dimensions. Ultrasound in Medicine and Biology. 1996; 22(8):979–986. [PubMed: 9004421]
28. Deng J, Rodeck CH. New fetal cardiac imaging techniques. Prenatal Diagnosis. 2004; 24(13): 1092–1103. [PubMed: 15614881]
29. Deng J, Yates R, et al. Dynamic three-dimensional color Doppler ultrasound of human fetal intracardiac flow. Ultrasound in Obstetrics & Gynecology. 2002; 20(2):131–136. [PubMed: 12153663]

30. DeVore GR, Falkensammer P, et al. Spatio-temporal image correlation (STIC): new technology for evaluation of the fetal heart. Ultrasound in Obstetrics & Gynecology. 2003; 22(4):380–387. [PubMed: 14528474]
31. Dhenain M, Ruffins SW, et al. Three-dimensional digital mouse atlas using high-resolution MRI. Developmental Biology. 2001; 232(2):458–470. [PubMed: 11401405]
32. Dimopoulos K, Diller GP, et al. Anemia in Adults With Congenital Heart Disease Relates to Adverse Outcome. Journal of the American College of Cardiology. 2009; 54(22):2093–2100. [PubMed: 19926019]
33. Dimopoulos K, Diller GP, et al. Prevalence, predictors, and prognostic value of renal dysfunction in adults with congenital heart disease. Circulation. 2008; 117(18):2320–2328. [PubMed: 18443238]
34. Dimopoulos K, Diller GP, et al. Hyponatraemia: a strong predictor of mortality in adults with congenital heart disease. European Heart Journal. 2010; 31(5):595–601. [PubMed: 19933692]
35. Faraj KA, Cuijpers V, et al. Micro-Computed Tomographical Imaging of Soft Biological Materials Using Contrast Techniques. Tissue Engineering Part C-Methods. 2009; 15(3):493–499. [PubMed: 19485760]
36. Filas BA, Varner VD, et al. Tracking Morphogenetic Tissue Deformations in the Early Chick Embryo. Journal of Visualized Experiments. 2011; 56
37. Foster FS, Zhang MY, et al. A new ultrasound instrument for in vivo microimaging of mice. Ultrasound in Medicine and Biology. 2002; 28(9):1165–1172. [PubMed: 12401387]
38. Furuse J, Maru Y, et al. Visualization of blood flow in hepatic vessels and hepatocellular carcinoma using B-flow sonography. Journal of Clinical Ultrasound. 2001; 29(1):1–6. [PubMed: 11180178]
39. Gardiner HM, Pasquini L, et al. Myocardial tissue Doppler and long axis function in the fetal heart. International Journal of Cardiology. 2006; 113(1):39–47. [PubMed: 16360223]
40. Godfrey ME, Messing B, et al. Fetal Cardiac Function: M-Mode and 4D Spatiotemporal Image Correlation. Fetal Diagnosis and Therapy. 2012; 32(1–2):17–21. [PubMed: 22777135]
41. Goncalves LF, Espinoza J, et al. Applications of 2-dimensional matrix array for 3-and 4-dimensional examination of the fetus - A pictorial essay. Journal of Ultrasound in Medicine. 2006; 25(6):745–755. [PubMed: 16731891]
42. Gorelick PB, Scuteri A, et al. Vascular Contributions to Cognitive Impairment and Dementia A Statement for Healthcare Professionals From the American Heart Association/American Stroke Association. Stroke. 2011; 42(9):2672–2713. [PubMed: 21778438]
43. Gratton S, Pohlhaus P, et al. Nanofabricated Particles for Engineered Drug Therapies: A Preliminary Biodistribution Study of PRINT Nanoparticles. Journal of Controlled Release. 2007; 121(1–2)
44. Gregg CL, Butcher JT. Quantitative in vivo imaging of embryonic development: Opportunities and challenges. Differentiation. 2012; 84(1)
45. Guldberg RE, Ballock RT, et al. Analyzing bone, blood vessels, and biomaterials with microcomputed tomography. Ieee Engineering in Medicine and Biology Magazine. 2003; 22(5): 77–83. [PubMed: 14699940]
46. Hamburger V, Hamilton HL. A SERIES OF NORMAL STAGES IN THE DEVELOPMENT OF THE CHICK EMBRYO. Journal of Morphology. 1951; 88(1):49-&. [PubMed: 24539719]
47. Henning AL, Jiang MX, et al. Quantitative Three-Dimensional Imaging of Live Avian Embryonic Morphogenesis Via Micro-computed Tomography. Developmental Dynamics. 2011; 240(8):1949–1957. [PubMed: 21761480]
48. Herberg U, Steinweg B, et al. Echocardiography in the Fetus - A Systematic Comparative Analysis of Standard Cardiac Views with 2D, 3D Reconstructive and 3D Real-Time Echocardiography. Ultraschall in Der Medizin. 2011; 32(3):293–301. [PubMed: 20425686]
49. Hoffman JIE, Kaplan S. The incidence of congenital heart disease. Journal of the American College of Cardiology. 2002; 39(12):1890–1900. [PubMed: 12084585]
50. Hogers B, van der Weerd L, et al. Non-invasive tracking of avian development in vivo by MRI. Nmr in Biomedicine. 2009; 22(4):365–373. [PubMed: 19003815]

51. Holmes WM, McCabe C, et al. Noninvasive self-gated magnetic resonance cardiac imaging of developing chick embryos in ovo. Circulation. 2008; 117(21):E346–E347. [PubMed: 18506012]
52. Hornberger LK, Sanders SP, et al. LEFT-HEART OBSTRUCTIVE LESIONS AND LEFT-VENTRICULAR GROWTH IN THE MIDTRIMESTER FETUS - A LONGITUDINAL-STUDY. Circulation. 1995; 92(6):1531–1538. [PubMed: 7664437]
53. Hornberger LK, Sanders SP, et al. IN-UTERO PULMONARY-ARTERY AND AORTIC GROWTH AND POTENTIAL FOR PROGRESSION OF PULMONARY OUTFLOW TRACT OBSTRUCTION IN TETRALOGY OF FALLOT. Journal of the American College of Cardiology. 1995; 25(3):739–745. [PubMed: 7860923]
54. Huang GY, Wessels A, et al. Alteration in connexin 43 gap junction gene dosage impairs conotruncal heart development. Developmental Biology. 1998; 198(1):32–44. [PubMed: 9640330]
55. Jenkins MW, Peterson L, et al. Measuring hemodynamics in the developing heart tube with four-dimensional gated Doppler optical coherence tomography. Journal of Biomedical Optics. 2010; 15(6)
56. Ji RP, Phoon CKL. Noninvasive localization of nuclear factor of activated T cells c1−/− mouse embryos by ultrasound biomicroscopy-Doppler allows genotype-phenotype correlation. Journal of the American Society of Echocardiography. 2005; 18(12):1415–1421. [PubMed: 16376776]
57. Johnson JT, Hansen MS, et al. Virtual histology of transgenic mouse embryos for high-throughput phenotyping. Plos Genetics. 2006; 2(4):471–477.
58. Kim JS, Min JH, et al. Quantitative Three-Dimensional Analysis of Embryonic Chick Morphogenesis Via Microcomputed Tomography. Anatomical Record-Advances in Integrative Anatomy and Evolutionary Biology. 2011; 294(1):1–10.
59. Kleinman CS, Hobbins JC, et al. ECHOCARDIOGRAPHIC STUDIES OF THE HUMAN-FETUS - PRENATAL-DIAGNOSIS OF CONGENITAL HEART-DISEASE AND CARDIAC DYSRHYTHMIAS. Pediatrics. 1980; 65(6):1059–1067. [PubMed: 7375228]
60. Kowalski W, Teslovich N, et al. Computational hemodynamic optimization predicts dominant aortic arch selection is driven by embryonic outflow tract orientation in the chick embryo. Biomechanics and Modeling in Mechanobiology. 2012; 11(7):1057–1073. [PubMed: 22307681]
61. Kowalski WJ, Dur O, et al. Critical Transitions in Early Embryonic Aortic Arch Patterning and Hemodynamics. Plos One. 2013; 8(3)
62. Le Floc'h J, Cherin E, et al. Developmental changes in integrated ultrasound backscatter from embryonic blood in vivo in mice at high us frequency. Ultrasound in Medicine and Biology. 2004; 30(10):1307–1319. [PubMed: 15582230]
63. Liebling M, Forouhar AS, et al. Four-dimensional cardiac imaging in living embryos via postacquisition synchronization of nongated slice sequences. Journal of Biomedical Optics. 2005; 10(5)
64. Lieu D. Ultrasound Physics and Instrumentation for Pathologists. Archives of Pathology & Laboratory Medicine. 2010; 134(10):1541–1556. [PubMed: 20923312]
65. Lindsey SE, Butcher JT. The cycle of form and function in cardiac valvulogenesis. Aswan Heart Centre Science & Practice Series. 2011; 2011(2):10.
66. Litzlbauer HD, Neuhaeuser C, et al. Three-dimensional imaging and morphometric analysis of alveolar tissue from microfocal X-ray-computed tomography. American Journal of Physiology-Lung Cellular and Molecular Physiology. 2006; 291(3):L535–L545. [PubMed: 16679382]
67. Liu AP, Wang RK, et al. Efficient postacquisition synchronization of 4-D nongated cardiac images obtained from optical coherence tomography: application to 4-D reconstruction of the chick embryonic heart. Journal of Biomedical Optics. 2009; 14(4)
68. Liu AP, Wang RKK, et al. Dynamic variation of hemodynamic shear stress on the walls of developing chick hearts: computational models of the heart outflow tract. Engineering with Computers. 2009; 25(1):73–86.
69. Liu W, Frank JA. Detection and quantification of magnetically labeled cells by cellular MRI. European Journal of Radiology. 2009; 70(2):258–264. [PubMed: 18995978]
70. Luo W, Marks DL, et al. Three-dimensional optical coherence tomography of the embryonic murine cardiovascular system. Journal of Biomedical Optics. 2006; 11(2)

71. Manner J, Thrane L, et al. In Vivo Imaging of the Cyclic Changes in Cross-sectional Shape of the Ventricular Segment of Pulsating Embryonic Chick Hearts at Stages 14 to 17: A Contribution to the Understanding of the Ontogenesis of Cardiac Pumping Function. Developmental Dynamics. 2009; 238(12):3273–3284. [PubMed: 19924823]
72. Maulik D, Nanda NC, et al. Live three-dimensional echocardiography of the human fetus. Echocardiography-a Journal of Cardiovascular Ultrasound and Allied Techniques. 2003; 20(8): 715–721.
73. McElhinney DB, Marshall AC, et al. Predictors of Technical Success and Postnatal Biventricular Outcome After In Utero Aortic Valvuloplasty for Aortic Stenosis With Evolving Hypoplastic Left Heart Syndrome. Circulation. 2009; 120(15):1482–U1448. [PubMed: 19786635]
74. Metscher BD. MicroCT for comparative morphology: simple staining methods allow high-contrast 3D imaging of diverse non-mineralized animal tissues. BMC Physiology. 2009; 9:11. [PubMed: 19545439]
75. Metscher BD. MicroCT for Developmental Biology: A Versatile Tool for High-Contrast 3D Imaging at Histological Resolutions. Developmental Dynamics. 2009; 238(3):632–640. [PubMed: 19235724]
76. Meyer-Wittkopf M, Cooper S, et al. Three-dimensional (3D) echocardiographic analysis of congenital heart disease in the fetus: comparison with cross-sectional (2D) fetal echocardiography. Ultrasound in Obstetrics & Gynecology. 2001; 17(6):485–492. [PubMed: 11422968]
77. Nelson TR. Three-dimensional fetal echocardiography. Progress in Biophysics & Molecular Biology. 1998; 69(2–3):257–272. [PubMed: 9785942]
78. Nelson TR, Pretorius DH, et al. Three-dimensional echocardiographic evaluation of fetal heart anatomy and function: Acquisition, analysis, and display. Journal of Ultrasound in Medicine. 1996; 15(1):1–9. [PubMed: 8667477]
79. Nieman BJ, Szulc KU, et al. Three-Dimensional, In Vivo MRI With Self-Gating and Image Coregistration in the Mouse. Magnetic Resonance in Medicine. 2009; 61(5):1148–1157. [PubMed: 19253389]
80. Oosterbaan AM, Ursem NTC, et al. Doppler flow velocity waveforms in the embryonic chicken heart at developmental stages corresponding to 5–8 weeks of human gestation. Ultrasound in Obstetrics & Gynecology. 2009; 33(6):638–644. [PubMed: 19434670]
81. Petiet AE, Kaufman MH, et al. High-resolution magnetic resonance histology of the embryonic and neonatal mouse: A 4D atlas and morphologic database. Proceedings of the National Academy of Sciences of the United States of America. 2008; 105(34):12331–12336. [PubMed: 18713865]
82. Phoon CKL, Aristizabal O, et al. 40 MHz Doppler characterization of umbilical and dorsal aortic blood flow in the early mouse embryo. Ultrasound in Medicine and Biology. 2000; 26(8):1275–1283. [PubMed: 11120365]
83. Phoon CKL, Ji RP, et al. Embryonic heart failure in NFATc1(−/−) mice - Novel mechanistic insights from in utero ultrasound biomicroscopy. Circulation Research. 2004; 95(1):92–99. [PubMed: 15166096]
84. Pierpont ME, Basson CT, et al. Genetic basis for congenital heart defects: Current knowledge - A scientific statement from the American heart association congenital cardiac defects committee, council on cardiovascular disease in the young. Circulation. 2007; 115(23):3015–3038. [PubMed: 17519398]
85. Rajiah P, Mak C, et al. Ultrasound of Fetal Cardiac Anomalies. American Journal of Roentgenology. 2011; 197(4):W747–W760. [PubMed: 21940548]
86. Roest AAW, de Roos A. Imaging of patients with congenital heart disease. Nature Reviews Cardiology. 2012; 9(2):101–115.
87. S J, D B, et al. Microfluidic Characterization of Cilia-Driven Fluid Flow Using Optical Coherence Tomography-Based Particle Tracking Velocimetry. Biomedical Optics Express. 2011; 2(7):2022–2034. [PubMed: 21750777]
88. Samanek M. CHILDREN WITH CONGENITAL HEART-DISEASE - PROBABILITY OF NATURAL SURVIVAL. Pediatric Cardiology. 1992; 13(3):152–158. [PubMed: 1603715]
89. Schneider JE, Bamforth SD, et al. Rapid identification and 3D reconstruction of complex cardiac malformations in transgenic mouse embryos using fast gradient echo sequence magnetic resonance

imaging. Journal of Molecular and Cellular Cardiology. 2003; 35(2):217–222. [PubMed: 12606262]

90. Seidl AH, Sanchez JT, et al. Transgenic quail as a model for research in the avian nervous system: A comparative study of the auditory brainstem. Journal of Comparative Neurology. 2013; 521(1): 5–23. [PubMed: 22806400]
91. Sklansky M. Advances in fetal cardiac imaging. Pediatric Cardiology. 2004; 25(3):307–321. [PubMed: 15360121]
92. Sklansky MS, Nelson TR, et al. Usefulness of gated three-dimensional fetal echocardiography to reconstruct and display structures not visualized with two-dimensional imaging. American Journal of Cardiology. 1997; 80(5):665-&. [PubMed: 9295008]
93. Sklansky MS, Nelson TR, et al. Real-time three-dimensional fetal echocardiography: Initial feasibility study. Circulation. 1999; 100(18):394–394.
94. Small M, Copel JA. Indications for fetal echocardiography. Pediatric Cardiology. 2004; 25(3):210–222. [PubMed: 15360114]
95. Srinivasan S, Baldwin HS, et al. Noninvasive, in utero imaging of mouse embryonic heart development with 40-MHz echocardiography. Circulation. 1998; 98(9):912–918. [PubMed: 9738647]
96. Stekelenburg-De Vos S, Steendijk P, et al. Systolic and diastolic ventricular function assessed by pressure-volume loops in the stage 21 venous clipped chick embryo. Pediatric Research. 2005; 57(1):16–21. [PubMed: 15531737]
97. Stekelenburg-de Vos S, Steendijk P, et al. Systolic and diastolic ventricular function in the normal and extra-embryonic venous clipped chicken embryo of stage 24: a pressure-volume loop assessment. Ultrasound in Obstetrics & Gynecology. 2007; 30(3):325–331. [PubMed: 17721868]
98. Stekelenburg-de Vos S, Ursem NTC, et al. Acutely altered hemodynamics following venous obstruction in the early chick embryo. Journal of Experimental Biology. 2003; 206(6):1051–1057. [PubMed: 12582147]
99. Stoll C, Alembik Y, et al. Evaluation of prenatal diagnosis of congenital heart disease. Prenatal Diagnosis. 1998; 18(8):801–807. [PubMed: 9742567]
100. Sydorak RM, Nijagal A, et al. Endoscopic techniques in fetal surgery. Yonsei Medical Journal. 2001; 42(6):695–710. [PubMed: 11754153]
101. Turnbull DH, Mori S. MRI in mouse developmental biology. Nmr in Biomedicine. 2007; 20(3): 265–274. [PubMed: 17451170]
102. Tworetzky W, McElhinney DB, et al. Improved surgical outcome after fetal diagnosis of hypoplastic left heart syndrome. Circulation. 2001; 103(9):1269–1273. [PubMed: 11238272]
103. Ursem NT, de Vos S, et al. Ventricular diastolic filling characteristics in the stage 24 chick embryo after vitelline vein obstruction. FASEB Journal. 2002; 16(5):A1126–A1127.
104. Ursem NTC, Struijk PC, et al. Dorsal aortic flow velocity in chick embryos of stage 16 to 28. Ultrasound in Medicine and Biology. 2001; 27(7):919–924. [PubMed: 11476925]
105. Votino C, Jani J, et al. Magnetic resonance imaging in the normal fetal heart and in congenital heart disease. Ultrasound in Obstetrics & Gynecology. 2012; 39(3):322–329. [PubMed: 21837757]
106. Wadghiri YZ, Schneider AE, et al. Contrast-enhanced MRI of right ventricular abnormalities in Cx43 mutant mouse embryos. Nmr in Biomedicine. 2007; 20(3):366–374. [PubMed: 17451172]
107. Wang XF, Deng YB, et al. Live three-dimensional echocardiography: Imaging principles and clinical application. Echocardiography-a Journal of Cardiovascular Ultrasound and Allied Techniques. 2003; 20(7):593–604.
108. Wu HM, Zhang Y, et al. Novel Application of Four-Dimensional Sonography with B-Flow Imaging and Spatiotemporal Image Correlation in the Assessment of Fetal Congenital Heart Defects. Echocardiography-a Journal of Cardiovascular Ultrasound and Allied Techniques. 2012; 29(5):614–619.
109. Xiong Y, Chen M, et al. A novel way of visualizing the ductal and aortic arches by real-time three-dimensional ultrasound with live xPlane imaging. Ultrasound in Obstetrics & Gynecology. 2012; 39(3):316–321. [PubMed: 21710662]

110. Xiong Y, Chen M, et al. Scan the fetal heart by real-time three-dimensional echocardiography with live xPlane imaging. Journal of Maternal-Fetal & Neonatal Medicine. 2012; 25(4):324–328. [PubMed: 21574902]

111. Xiong Y, Liu T, et al. Comparison of real-time three-dimensional echocardiography and spatiotemporal image correlation in assessment of fetal interventricular septum. Journal of Maternal-Fetal & Neonatal Medicine. 2012; 25(11):2333–2338. [PubMed: 22642553]

112. Xu Z, Owens G, et al. Noninvasive Creation of an Atrial Septal Defect by Histotripsy in a Canine Model. Circulation. 2010; 121(6):742–749. [PubMed: 20124126]

113. Yagel S, Arbel R, et al. The three vessels and trachea view (3VT) in fetal cardiac scanning. Ultrasound in Obstetrics & Gynecology. 2002; 20(4):340–345. [PubMed: 12383314]

114. Yagel S, Cohen SM, et al. 3D and 4D ultrasound in fetal cardiac scanning: a new look at the fetal heart. Ultrasound in Obstetrics & Gynecology. 2007; 29(1):81–95. [PubMed: 17200988]

115. Yalcin HC, Shekhar A, et al. Hemodynamic Patterning of the Avian Atrioventricular Valve. Developmental Dynamics. 2011; 240(1):23–35. [PubMed: 21181939]

116. Yalcin HC, Shekhar A, et al. Two-photon microscopy-guided femtosecond-laser photoablation of avian cardiogenesis: noninvasive creation of localized heart defects. American Journal of Physiology-Heart and Circulatory Physiology. 2010; 299(5):H1728–H1735. [PubMed: 20709864]

117. Yang QH, Khoury MJ, et al. Trends and patterns of mortality associated with birth defects and genetic diseases in the United States, 1979–1992: An analysis of multiple-cause mortality data. Genetic Epidemiology. 1997; 14(5):493–505. [PubMed: 9358267]

118. Yoo J, Larina IV, et al. Increasing the Field-of-View of Dynamic Cardiac OCT via Post-Acquisition Mosaicing Without Affecting Frame-Rate or Spatial Resolution. Biomedical Optics Express. 2011; 2(9):2614–2622. [PubMed: 22091446]

119. Zabadneh N, Santagati C, et al. Usefulness of Fetal Three-Dimensional Ultrasonography for Detecting of Congenital Heart Defects and Associated Syndromes. Pediatric Cardiology. 2011; 32(6):724–736. [PubMed: 21479665]

120. Zhou YQ, Foster FS, et al. Developmental changes in left and right ventricular diastolic filling patterns in mice. American Journal of Physiology-Heart and Circulatory Physiology. 2003; 285(4):H1563–H1575. [PubMed: 12805021]

121. Zhou YQ, Foster FS, et al. Applications for multifrequency ultrasound biomicroscopy in mice from implantation to adulthood. Physiological Genomics. 2002; 10(2):113–126. [PubMed: 12181368]

122. Zhu XY, Bentley MD, et al. Early changes in coronary artery wall structure detected by microcomputed tomography in experimental hypercholesterolemia. American Journal of Physiology-Heart and Circulatory Physiology. 2007; 293(3):H1997–H2003. [PubMed: 17573460]

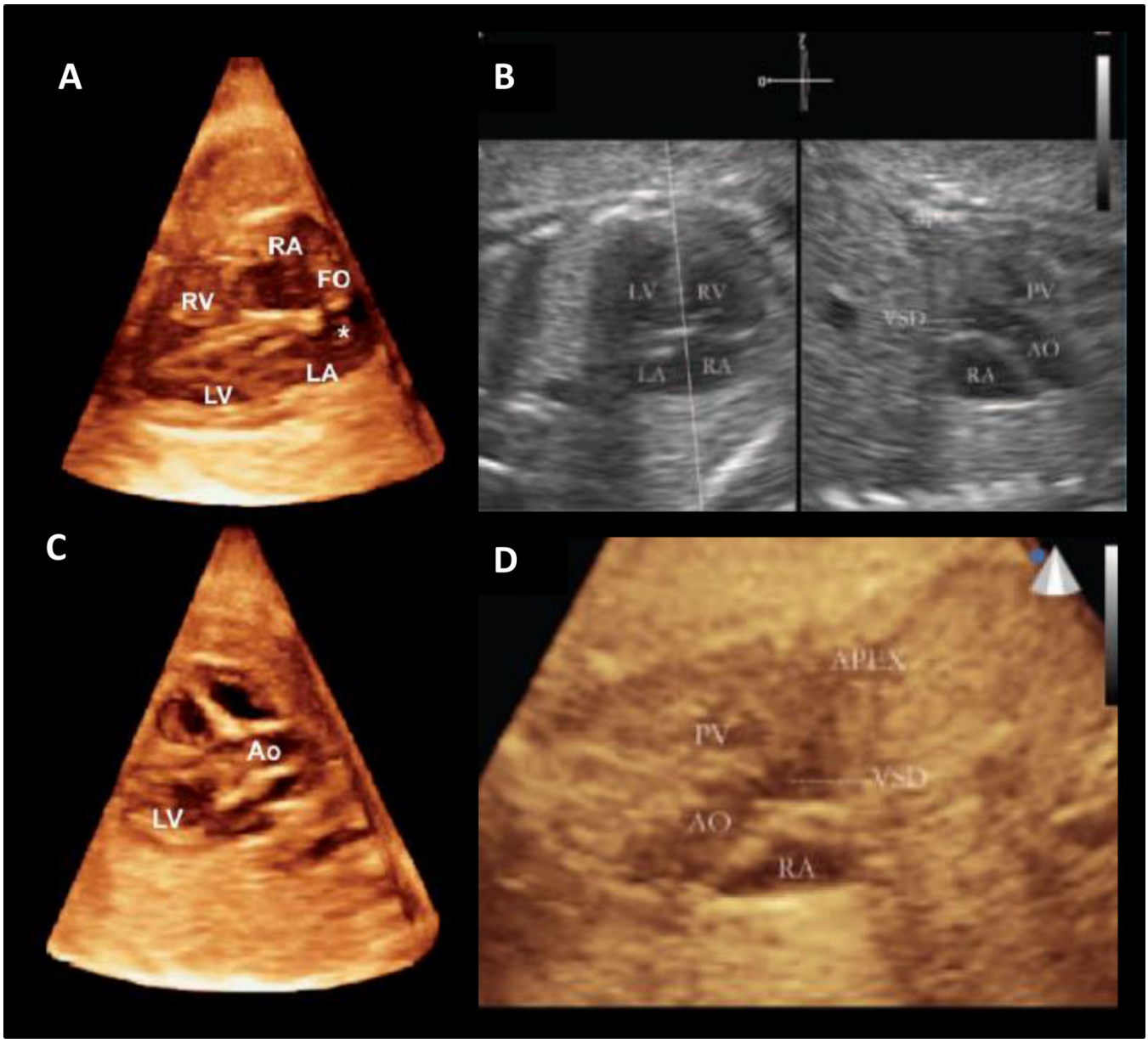

Figure 1.

Live 3D/4D Clinical Ultrasound Imaging: 3D rendered volume using real time 3D ultrasound of a fetus at 33 weeks displaying the four chamber view (A) and the left ventricular outflow tract with aortic valve (C) (Herberg, Steinweg et al. 2011), Ventricular septal defect (VSD) visualized through 3D ultrasound with live xPlane imaging (B) and live 3D ultrasound imaging of the VSD (D) (Xiong, Liu et al. 2012)

LV = left ventricle, RV = right venricle, Ao = aorta, LA = left atrium, RA = right atrium, FO = foramen ovale

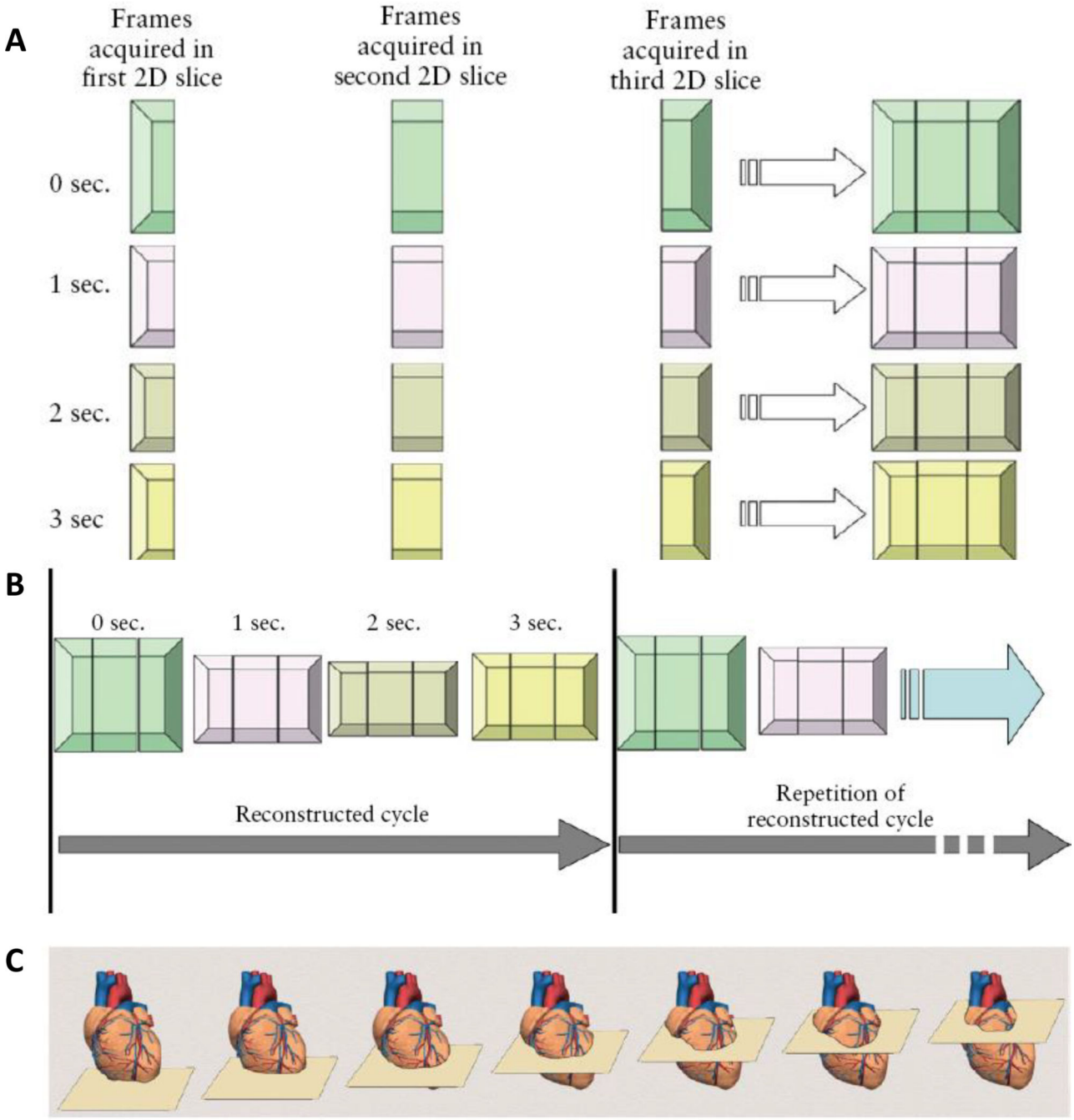

Figure 2.

Schematic of Spatiotemporal Image Correlation Technology: Based on a simplified number of slices, frames per slice, and cycle duration, the heart is scanned in three consecutive slices over time (A), STIC reconstructs consecutive cycles generating a transient volume representing real time 3D ultrasound (B), multiple slices of the heart are acquired during a single ultrasound scan with STIC (C) (Yagel, Cohen et al. 2007)

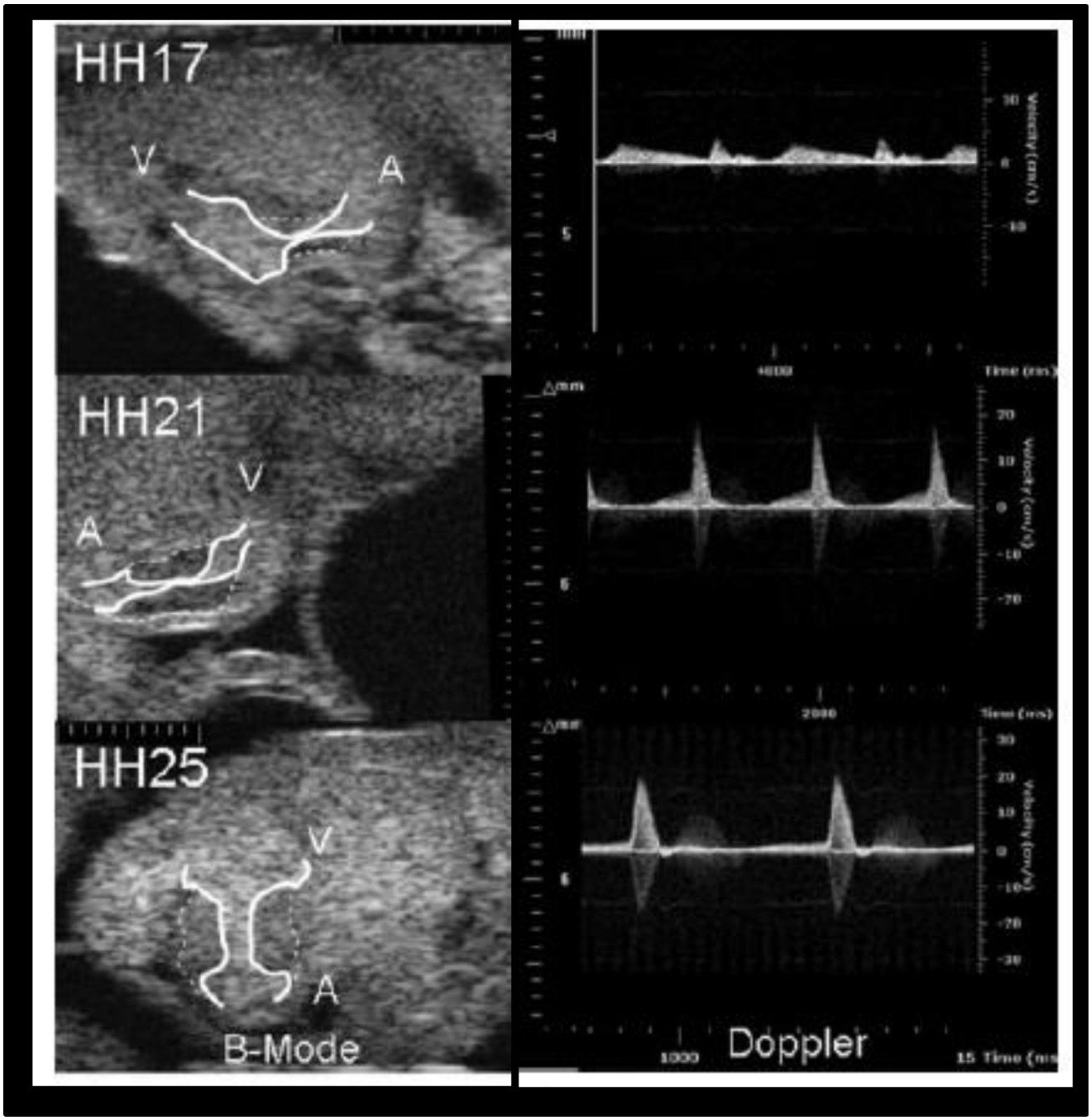

Figure 3.

Atrioventricular canal visualized with ultrasound biomicroscopy (55MHz) through different stages of cardiac development (C), Doppler ultrasound through the atrioventricular canal during development (Butcher, McQuinn et al. 2007)

Scale Marks = 100μm

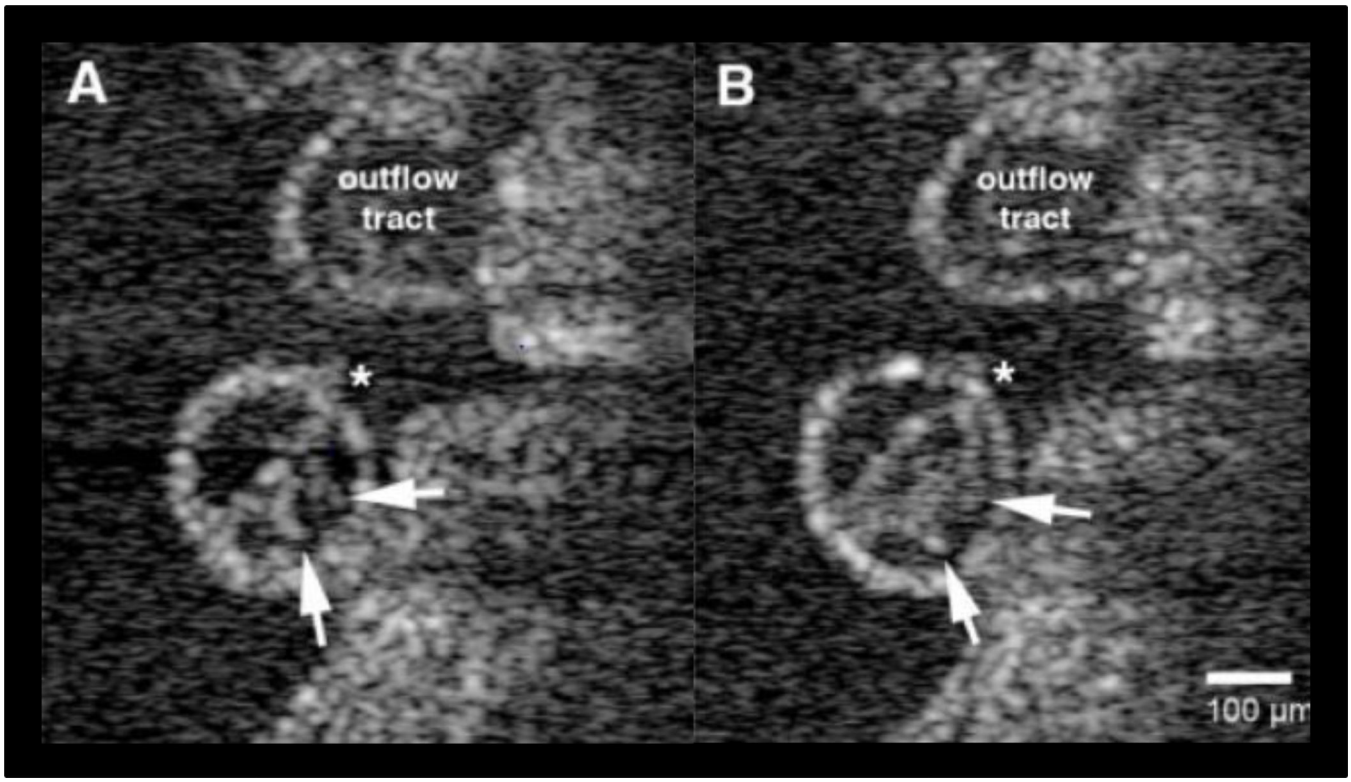

Figure 4.

Cross sections of the ventricle in embryonic chick hearts visualized with OCT where endocardial spikes (arrows) are seen on the endocardial tube that is emptied (A) and filled (B) with blood during the heart beat (Manner et al 2009)

Scale bar = 100µm *inner curvature

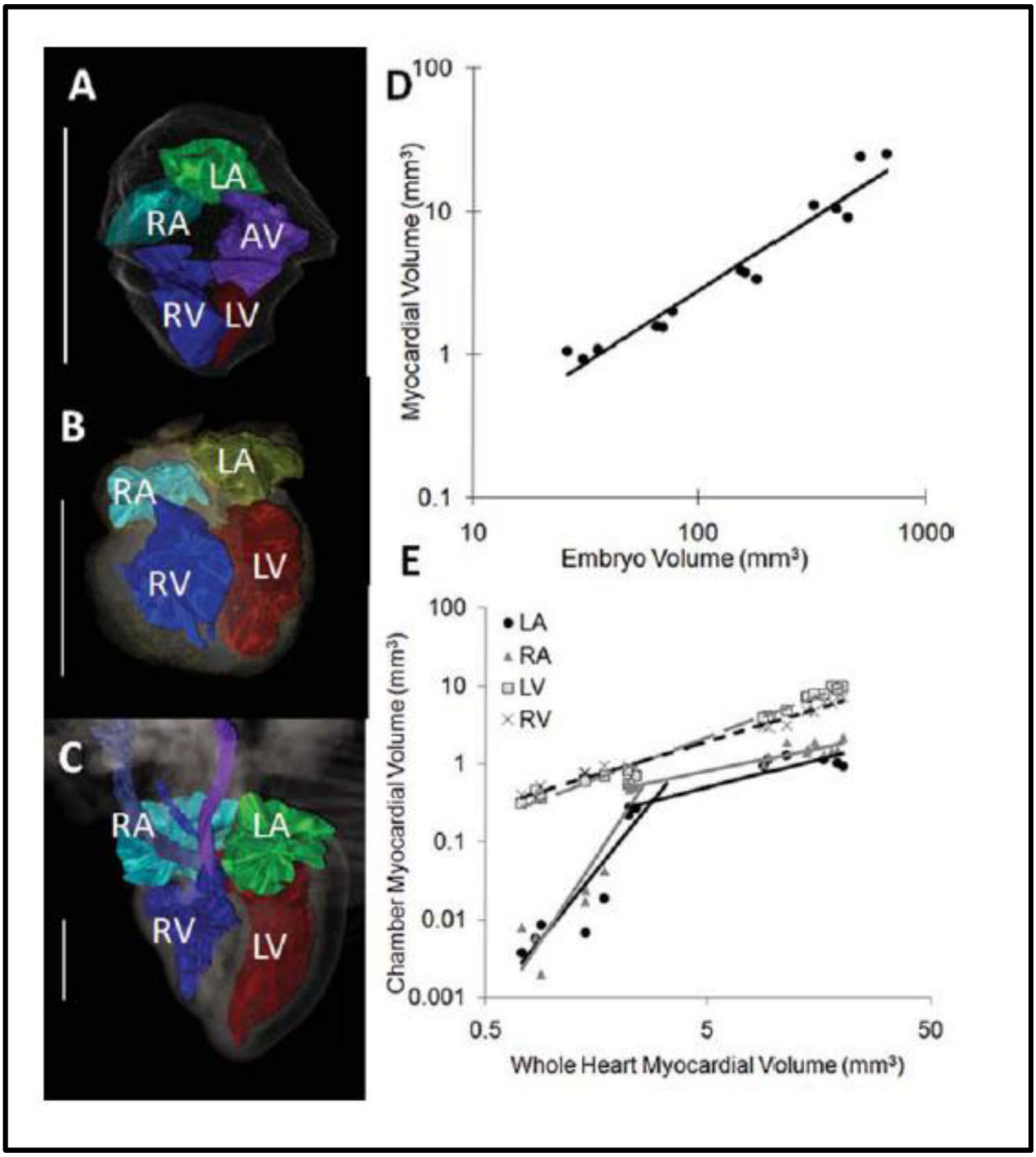

Figure 5.

3D segmentation and quantiative analysis of the chick heart after microCT imaging at Day 4(A), Day 7(B), and Day (C) of development, Mathematical relationships of the myocardial volume compared to the entire embyro volume (D), and the chamber specific myocardial volume as compared to the whole heart volume (E)(Kim, Min et al. 2011)

Scale Bar = 1mm, LA = left atrium, LV = left ventricle, RA = right atrium, RV = right ventricle

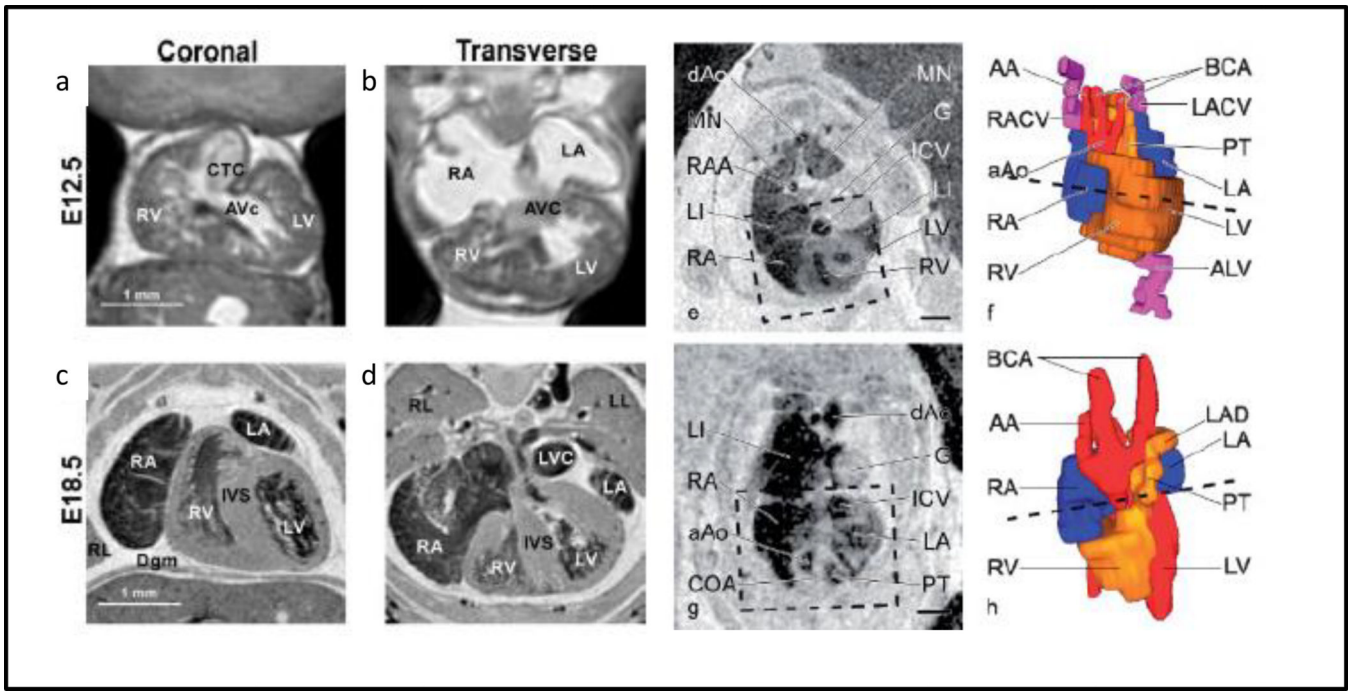

Figure 6.

3D MRI scans (3 hrs) of extracted and fixed embryonic mice with spatial resolution of 19.5μm at E12.5 coronal slice (a), E12.5 transverse slice (b), E18.5 coronal slice (c), E18.5 transverse slice (d) (Petiet, Kaufman et al. 2008). Chick embryos imaged with MRI and 3D reconstructed at day 7 (e,f) and day 10 (g,h). The box represents the area that was reconstructed and the dashed lines show the level of the MRI slice (Hogers, van der Weerd et al. 2009)

Scale bars = 1mm

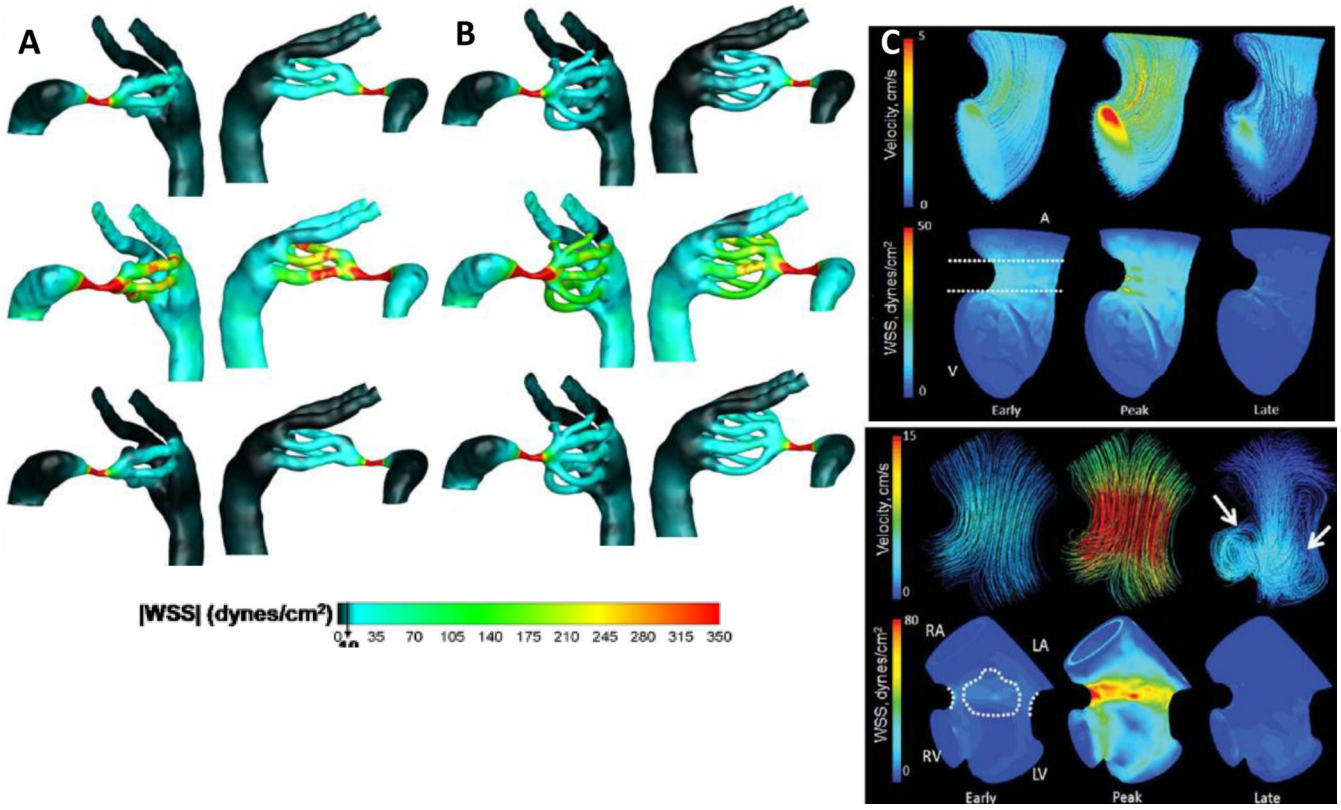

Figure 7.

Aortic arch WSS distributions found from CFD simulations for stage 21 chicks for a 2 aortic arch configuration (A) and 4 aortic arch configuration (B) (Kowalski, Dur et al. 2013). Acceleration, peak, and deceleration phases in the cardiac cycle are depicted in the CFD simulation data and the color scale ranges from 0–350 dynes/cm^2. CFD simulations showing the 3D hemodynamic environment in the atrioventricular region of the embryonic chick at HH17 (top) and HH23 (bottom). Arrows represent locations of vortices in the flow. Color legend in HH17 chicks show velocities ranging from 0–5cm/s and WSS ranging from 0–50 dynmes/cm^2. Color legend in HH23 chicks show velocities rangring from 0–15cm/s and WSS ranging from 0–80dynes/cm^2(Yalcin, Shekhar et al. 2011)

Table 1

Comparison of Embryonic Imaging Systems adapted from (Kim, Min et al. 2011)

Modality	Resolution (μm)	Depth of Field	Capital Cost	Operational Cost	Acquisition Time	Contrast Agents
Ultrasound/Biomicroscopy	30	3–4 mm	$$	$	N/A	No
OCT	1	1–3mm	$	N/A	12 hrs.	No
MicroCT	<1–25	<1–8 cm	$$$	$$	0.05–5 hrs.	Yes
MRI	25–100	>10 cm	$$$$$	$$$	6–30 hrs	Yes

Birth Defects Res C Embryo Today. Author manuscript; available in PMC 2015 June 18.

Table 2

Comparisons in Heart Development Across Animal Models adapted from (Lindsey and Butcher 2011)

Human (days)	Murine (embryonic days)	Avian (HH)	Description of Events
22	7–8	7	Fusion of paired heart tubes
22	7.5–8.5	7–10	Myocardial contractions begin and cardiac looping (mouse E8.5)
24	8–8.5	9–12+	Blood begins to flow through the heart
26	9–11	11–12	First ventricular trebeculations
28	10–12	13–22	Endocardial cushions can be defined (chick HH28)
29	11–13.5	15–23	First appearance atrial septum prium
31	12	24–28	Appearance of primordia semilunar valves, start AV septation
33	12–13	25–28	Completion of anterior-posterior septum
35	13–15	26–31	Completion of intraventricular septation
37–43		27–34	Maturation of semilunar valves